Polymer Journal, Vol. 28, No. 12, pp 1065—1070 (1996)

Viscoelastic Properties of Poly(2-vinylpyridine) in Bulk and Solution

Yoshiaki TAKAHASHI, Nobuo OCHIAI,* Yushu MATSUSHITA,** and Ichiro NODA

Department of Applied Chemistry, Nagoya University, Chikusa-ku, Nagoya 464-01, Japan

(Received May 16, 1996)

ABSTRACT: Viscoelastic properties of poly(2-vinylpyridine) (P2VP) over a wide range of molecular weight (M) were studied in bulk and solution. It was found that the absolute values of zero-shear viscosity η^0 of P2VP in bulk and in α-chloronaphtharene (αCN) are practically the same as those of polystyrene (PS) over whole experimental range of M. The temperature dependence of η^0 in bulk is also the same. It is concluded that among various polymers so far studied, P2VP and PS have very similar viscoelastic properties in both bulk and a good solvent (αCN), though the plateau modulus G_N^0 and steady state compliance J_e of P2VP are slightly different from those of PS.

KEY WORDS Poly(2-vinylpyridine) / Zero-Shear Viscosity / Plateau Modulus / Steady State Compliance /

Poly(2-vinylpyridine) (P2VP) homopolymers[1] with narrow molecular weight distributions and well defined block copolymers containing P2VP block, such as poly(styrene-*block*-2-vinylpyridine)[2] (PS–P2VP) can be prepared by anionic living polymerization technique over a wide range of molecular weight.

Matsushita *et al.*[1-4] studied dilute solution properties of P2VP and PS–P2VP diblock copolymers and reported that P2VP and PS have almost the same Kuhn segment length, chain conformation of PS–P2VP diblock copolymers in a common good solvent is similar to that of P2VP or PS in good solvents, and the conformation of PS part of PS–P2VP diblock copolymer is not affected by the existence of another block chain.

Recently, shear effects on order–disorder transition and microdomain structures of block copolymers, and also their viscoelastic properties become of interest.[5] PS–P2VP diblock copolymers are one of the suitable samples for these studies because they have well-defined structures and almost the same molecular characteristics as mentioned above, but still segregate at a certain condition in the ordinary temperature range of experiments.

We already reported[6] that zero-shear viscosity of PS–P2VP diblock copolymers in a common good solvent in semidilute region can be expressed by the scaling law similar to that of PS in good solvents.[7-9] However, viscoelastic properties of P2VP have not been well studied in contrast to PS. In this work, therefore, we study viscoelastic properties of P2VP homopolymers in bulk and solution to obtain fundamental data of P2VP block component in PS–P2VP block copolymers.

EXPERIMENTAL

Four P2VP samples with high molecular weights used here are the same ones synthesized and used in previous works.[1-3] The rest of the samples was synthesized and characterized in this work by the same manner as in the previous works. In addition, glass transition temperatures T_g of all the samples were measured with a DSC Type 3100 of MAC Science Co., at a constant heating rate, 5°C min^{-1}. Molecular characteristics of the samples thus determined are listed in Table I.

Viscoelastic properties of P2VP were measured with a Mechanical Spectrometer RMS800 and a Fluid Spectrometer RFSII of Rheometric Scientific Inc. Most of measurements were carried out in oscillatory shear flow by the use of a parallel-plate geometry of either 2.5 cm or 5 cm diameter in both instruments. For VPL5 in bulk, steady shear flow measurements were also carried out with a RMS800 by the use of a cone-plate geometry of 5 cm diameter and 0.04 radian cone-angle.

Five low molecular weight ($M < 4 \times 10^4$) samples were employed to measure in bulk only, while VPK3 was employed to measure in solution only. Other samples were employed to measure in both bulk and solution. A solvent used is α-chloronaphtharene (αCN), which is known as a good solvent for PS[9] and also was found to be a good solvent for P2VP as described later. Temperatures of measurements were varied between 120°C and 190°C in bulk and between 18.5°C and 50°C in solution.

RESULTS

In Bulk

All the data of storage and loss moduli measured in oscillatory flow were shifted to reference temperature T_r (160°C) and the master curve was generated for each sample. Figure 1 shows semilogarithmic plots of temperature shift factor a_T, used in master curve generation, against temperature T. To avoid the complication in plots, the data for VPL1, VPK21, and VPK22 are not shown in this figure since they are the same as those of the higher molecular weight samples. All the a_T data except the data for the two low molecular weight samples (VPL7 and VPK8) at low temperature, compose a single line, which can be expressed by a WLF equation,

$$\log a_T = \frac{-C_1(T-T_r)}{(C_2+(T-T_r))} \quad (1)$$

* Present address: *Dai-ichi Kogyo Seiyaku Co., Ltd., 55, Nishi-shichijo, Higashikubocho, Shimogyo-ku, Kyoto 600, Japan.*
** Present address: *Neutron Scattering Laboratory, ISSP, the University of Tokyo, Shirakata 106-1, Tokai, Ibaraki 319-11, Japan.*

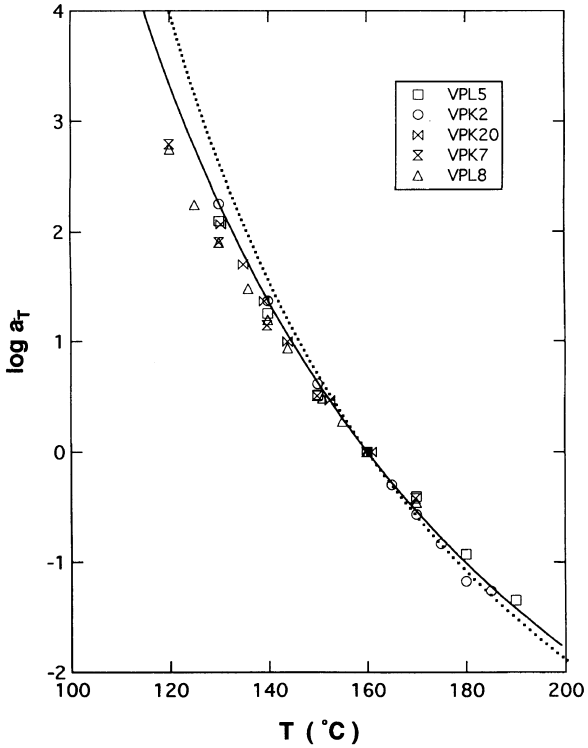

Figure 1. Semilogarithmic plots of temperature shift factor a_T against temperature T for P2VP in bulk. Symbols are denoted in the figure. Solid and dotted lines denote WLF equations (eq 1) for P2VP and PS, respectively. The reference temperature T_r is 160°C.

Table I. Molecular characteristics of poly(2-vinylpyridine)s

Sample	$M_w \times 10^{-4}$	M_w/M_n	T_g/°C	C^*/ kg dm^{-3}	$[\eta]$/ dm^3 kg^{-3}
VPK3	196	1.07		0.282	3.96
VPL5	67	1.12	102	0.656	1.81
VPK2	20.4	1.02		1.67	0.766
VPL1	9.4	1.12		3.05	0.431
VPK22	3.9	1.06	97	—	—
VPK20	3.7	1.06	98	—	—
VPK21	3.3	1.08	96	—	—
VPK7	1.7	1.44	88	—	—
VPL8	0.84	1.06	87	—	—

with $C_1 = 7.63$ and $C_2 = 131.9$.

As show in Table I, the T_g value becomes a constant for high molecular weight P2VP samples and is equal to that of high molecular weight PS measured with the same apparatus at the same heating rate. Therefore, the temperature dependencies of a_T of P2VP and PS can be compared at the same reference temperature. The WLF equation for PS at 160°C[10] is denoted by a dotted line in Figure 1. It is clear that both data are similar to each other, especially at high temperature region. The deviation of a_T values of low molecular weight samples from the WLF equation shown in Figure 1 is reasonable since these samples have lower T_g than other samples[10,11] (Table I).

Figure 2 shows the master curves of frequency (ω) dependence of storage (G') and loss (G') moduli at 160°C. No plateau region is observed for low molecular weight samples, VPL8 and VPK7 (not shown), while clear and broad plateau regions can be observed between terminal and transition regions for high molecular weight samples,

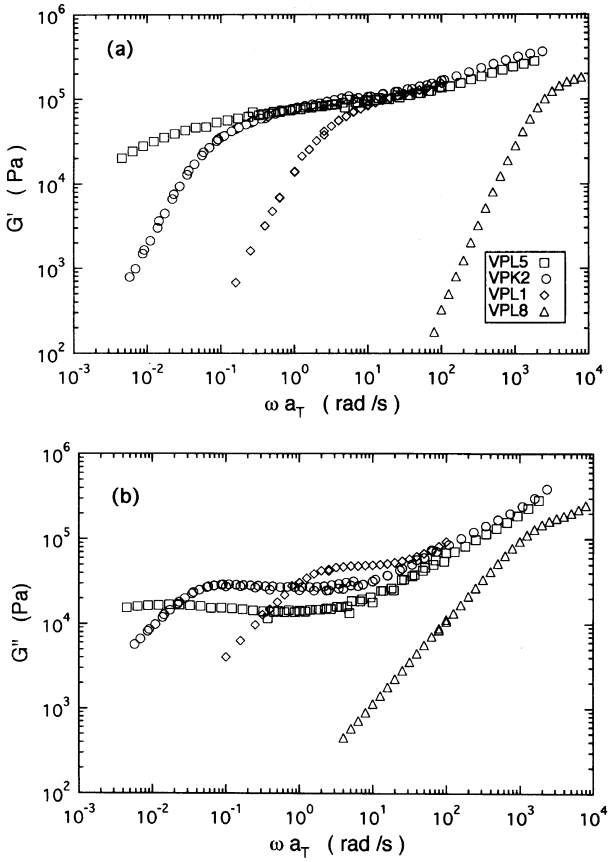

Figure 2. Double logarithmic plots of (a) G' and (b) G'' against ωa_T for P2VP in bulk at 160°C. Symbols are denoted in the figure (a).

VPL5 and VPK2. However, the G' values in plateau regions slightly but continuously increase with increase of frequency, so that the plateau modulus G_N^0 of P2VP cannot be determined from the G' behavior alone. The procedure of evaluation of plateau modulus will be described later.

From the data in terminal region, zero-shear viscosity η^0 and steady state compliance J_e were evaluated by ordinary methods,[11,12] as shown in Figure 3. η^0 of VPL1 and VPL8 were determined from the constant values of respective $\eta'(\omega)$ data approached at low ωa_T. However, $\eta'(\omega)$ of VPK2 did not become constant at low ωa_T, η^0 of this sample was obtained by extrapolating $\eta'(\omega)$ to low ωa_T, as denoted by a solid line in Figure 3a. J_e of these samples were also determined from the constant values of respective $J'(\omega)$ data approached at low ωa_T, neglecting one or two uncertain data at the lower end of ωa_T. η^0 and J_e for other samples in bulk were also determined by the same methods as those of VPL1 and VPL8.

For the highest molecular weight sample measured in bulk (VPL5), the terminal region behavior in oscillatory flow was not observed even at the highest experimental temperature (Figure 2). Therefore, η^0 and J_e of this sample was evaluated from steady shear flow measurements carried out at 180°C. Shear rate ($\dot{\gamma}$) dependence of $\eta(\dot{\gamma})$ and $J_S(\dot{\gamma})$ of VPL5 at 180°C are also shown in Figure 3. η^0 was determined from the constant value of $\eta(\dot{\gamma})$ approached at low $\dot{\gamma}$ and converted to the value at 160°C, by using eq 1. Only a limited numbers of $J_S(\dot{\gamma})$ data were obtained but all were almost constant, we

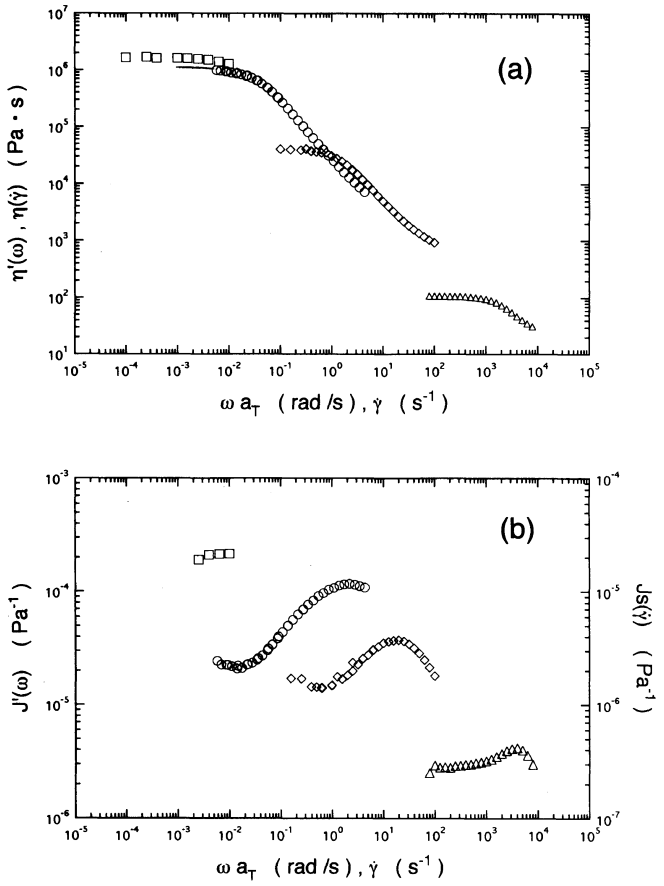

Figure 3. Double logarithmic plots of (a) $\eta'(\omega)$ *vs.* ωa_T at 160°C and $\eta(\dot{\gamma})$ *vs.* $\dot{\gamma}$ at 180°C, and (b) $J'(\omega)$ *vs.* ωa_T at 160°C and $J_S(\dot{\gamma})$ *vs.* $\dot{\gamma}$ at 180°C. Symbols are the same as those in Figure 2.

obtained J_e as an average of $J_S(\dot{\gamma})$ data neglecting the one at the lowest $\dot{\gamma}$, and converted to the value at 160°C.

It should be noted that η^0 and J_e of VPL5 and VPK2 have relatively larger experimental error (always larger in J_e) than the data for other samples due to their evaluation described above. However, from the fact that J_e of VPL5 and VPK2 in bulk are consistent with the data in solutions as shown later, we can safely assume that the error in these data do not seriously affect the results in this work.

Figures 4 and 5 show double logarithmic plots of η^0 and J_e at 160°C against weight-average molecular weight M_w, respectively. In Figure 4, the viscosity data of P2VP can be classified into two regions, *i.e.*, non-entangled and entangled regions denoted by dotted and solid lines, respectively. Molecular weight dependence of η^0 in the entangled region can be represented by 3.4th power of M_w. On the other hand, M_w dependence of η^0 in the non-entangled region is somewhat unclear. This is due to the fact that all the data are plotted at constant temperature instead of iso-free volume state.[10,11] There is difficulty in determining the critical molecular weight M_c for entanglement effects on η^0 accurately from this figure, but it is estimated to be between 3.5×10^4 and 4.5×10^4. This value is close to the M_w value where T_g starts to deviate from the constant value for high M_w samples and hence a_T deviates from the WLF equation. A similar tendency is reported for other polymers.[10,11]

Figure 5 shows that J_e values of P2VP can be classified into non-entangled and entangled regions. J_e is pro-

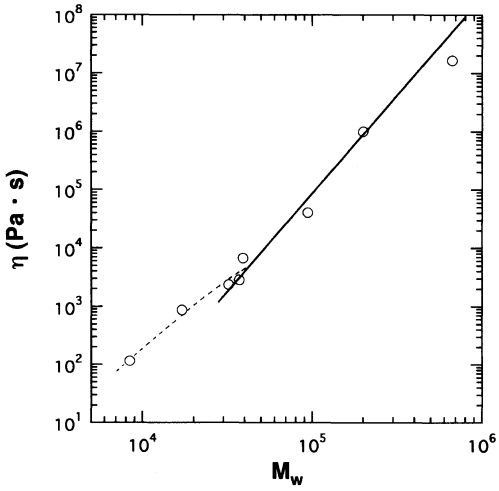

Figure 4. Double logarithmic plots of η_0 against M_w for P2VP in bulk at 160°C. Solid line denotes the slope of 3.4, while dotted line is drawn as a guide to show the lower M_w dependence in the non-entangle region.

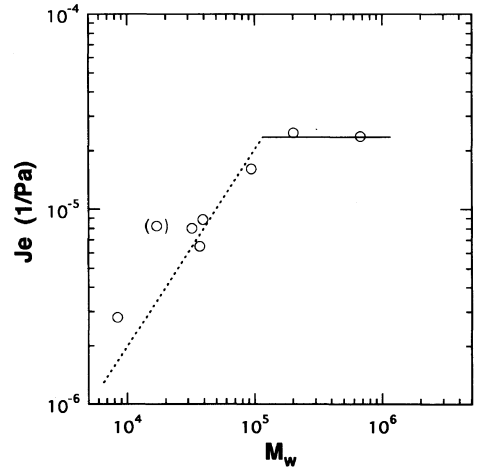

Figure 5. Double logarithmic plots of J_e against M_w for P2VP in bulk at 160°C. Dotted line denotes the slope of 1, while solid line denotes a constant value in the entangled region.

portional to M_w in the non-entangled region as denoted by a dotted line, while it is constant in the entangled region as denoted by a solid line. The critical molecular weight M_c' for entanglement effects on J_e is about 1×10^5, and the limiting value of J_e for high molecular weight samples is about 2.4×10^{-5} at 160°C. J_e value for VPK7 shown in parenthesis is much higher than the dotted line. This may be due to relatively wider molecular weight distribution of the sample as shown in Table I.[11,12] Thus, we neglect this datum in the following discussion.

In Solution

All the G' and G'' data measured in oscillatory flow were shifted to a reference temperature (30°C) and viscoelastic properties, η^0 and J_e at the temperature were evaluated in the same manner as in bulk.

Figure 6 shows double logarithmic plots of $\eta_{sp}^0/M_w^{3.4}$ against concentration C, where $\eta_{sp}^0 = (\eta^0 - \eta_s)/\eta_s$ is specific viscosity and η_s is solvent viscosity. Here, it is assumed that η_{sp}^0 is proportional to $M_w^{3.4}$ in the entangled regions, according to the results in bulk (Figure 4). As shown in Figure 6, all the data in the entangled region up to say, $C = 20\ \mathrm{kg\,dm^{-3}}$ compose a single straight line as denoted

by a solid line irrespective of molecular weight, while the concentration dependence become steeper at $C>20$ kg dm^{-3} as denoted by a broken line. On the other hand, a few data in the non-entangled region deviate from the straight line as denoted by a dotted line, indicating the lower concentration dependence. All these features of the η_{sp}^0 data of P2VP solutions are quite similar to those of PS solutions in good solvents.[9] Therefore, the data for P2VP solutions also can be classified into dilute, semidilute and concentrated regions. The behavior of η_{sp}^0 in respective regions are discussed later.

Figure 7 shows double logarithmic plots of J_e against C. The filled circle denotes the J_e value shifted to 30°C in bulk in the entangled region shown in Figure 5. It is clear that J_e data of P2VP solutions can be classified into non-entangled and entangled regions as other linear homopolymers.[11,12] J_e depends on M_w and it is inversely proportional to C as denoted by dotted lines in the non-entangled region, while J_e becomes independent of M_w and proportional to C^{-2} in the entangled region up to the bulk state.

DISCUSSION

As described above, the plateau modulus G_N^0 of P2VP cannot be determined from G' behavior alone. Therefore, the G_N^0 value in bulk was evaluated by the integration of G'' (eq 2)[10-12] for VPK2, in which the maximum was most clearly observed among all the samples,

$$G_{eN}^0 = \int_{-\infty}^{a} G'' \mathrm{d} \ln \omega \qquad (2)$$

where a is chosen to go across a maximum of G''. The G_N^0 value thus evaluated is 1.32×10^5 at 160°C. The corresponding critical molecular weight M_e evaluated by $M_e=\rho RT/G_N^0$, where ρ is density (1.08×10^3 kg m^{-3} at 160°C for P2VP[13]), is about 2.9×10^4.

All the critical molecular weights, the limiting value of J_e, and the G_N^0 value of P2VP in bulk determined in this study are tabulated in Table II, together with the corresponding data of PS.[10-12] The G_N^0 value of P2VP is somewhat lower than that of PS and consequently the M_e value of P2VP is somewhat higher than that of PS and M_c' value of P2VP is also somewhat lower than that of PS. However, all these values of P2VP are close to those of PS, compared to other bulk polymers studied so far.[12]

Moreover, the absolute values of a_T (Figure 1), η^0 (Figure 4), and J_e (Figure 5) are also close to those of PS, compared to other bulk polymers, though η^0 are slightly lower than, whereas J_e are slightly higher than those of PS,[10-12] respectively. On the whole, we conclude that viscoelastic properties of P2VP in bulk are very similar to those of PS.

In solution, the plateau region was observed only for

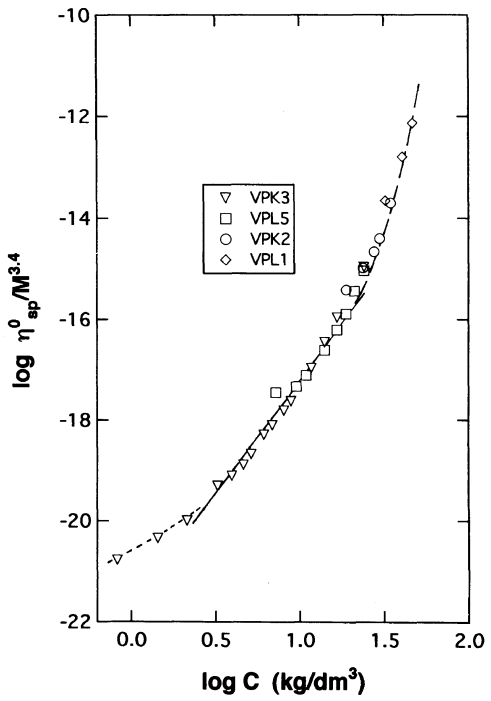

Figure 6. Double logarithmic plots of $\eta_{sp}^0/M^{3.4}$ against C for P2VP in αCN at 30°C. Symbols are denoted in the figure. Solid line denotes the slope calculated by eq 3b with $\nu=0.59_5$ in semidilute region. Dotted and broken lines denote the deviation from the solid line in dilute and concentrated regions, respectively.

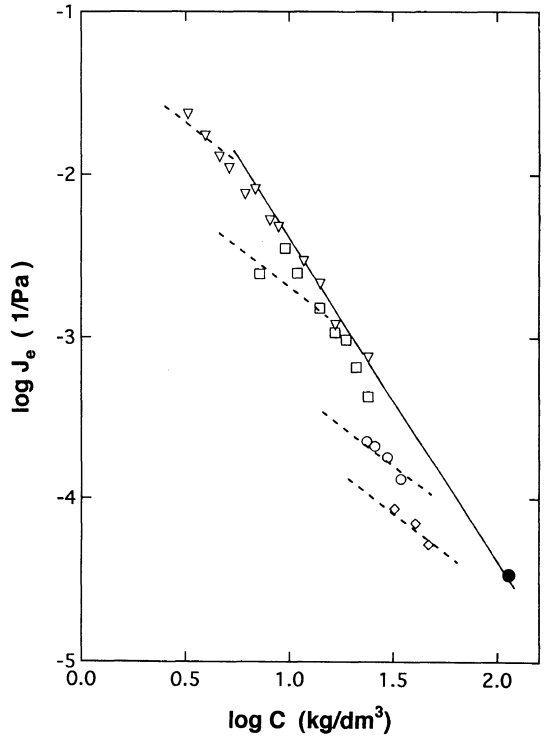

Figure 7. Double logarithmic plots of J_e against C for P2VP in αCN at 30°C. Symbols are the same as those in Figure 6. The filled circle denotes the value in bulk in the entangled region. Dotted and solid lines denote the slopes of -1 and -2, respectively.

Table II. Critical molecular weights and limiting values of J_e and G_N^0 at 160°C

	$M_e\times10^{-4}$	$M_c\times10^{-4}$	$M_c'\times10^{-4}$	J_e	G_N^0
Poly(2-vinylpyridine)	2.9	3.5–4.5	9–10	2.4×10^{-5}	$1.3_2\times10^5$
Polystyrene	1.8	3.3–4.0	13–14	1.9×10^{-5}	2.0×10^5

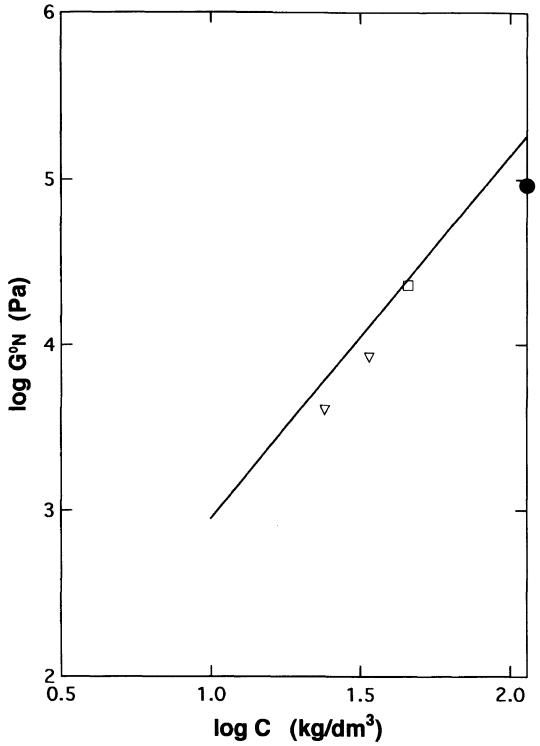

Figure 8. Double logarithmic plots of G_N^0 against C for P2VP in αCN at 30°C. Symbols are the same as those in Figure 6. The filled circle denotes the value in bulk. Solid line denotes the data for PS solutions, which have a slope nearly equal to 2.

the three highly concentrated solutions of high molecular weight samples and their G' values increase slightly but continuously, and the maxima in G'' do not clearly appear. Therefore, we assume that the value of G' where a very shallow minimum was observed in $\tan\delta$ corresponds to G_N^0. Figure 8 shows double logarithmic plots of plateau modulus G_N^0 against C. The value in bulk is converted to the value at 30°C and also plotted in this figure. It is clear that the G_N^0 value for P2VP are close to those of PS in good solvents[14] denoted by a solid line of which the slope is 2, though the data are scarce.

As reported in previous works,[8,9] the reduced zero-shear viscosity η_R^0 defined by $\eta_R^0 \equiv \eta_{sp}^0/C[\eta]$ where $[\eta]$ is intrinsic viscosity, can be expressed as a universal function of degree of coil overlapping C/C^* in dilute and semidilute regions, where $C^* = 3M/(4\pi\langle S^2\rangle^{3/2}N_A)$ is the critical concentration at which polymer coils begin to overlap with each other; η_R^0 is expressed by an expansion form of C/C^* in dilute region, and it can be expressed by scaling theory in semidilute region as

$$\eta_R^0 \propto (C/C^*)^{(4.4-3\nu)/(3\nu-1)} \tag{3a}$$

or

$$\eta_{sp}^0 \propto M^{3.4} C^{3.4/(3\nu-1)} \tag{3b}$$

where ν is exponent in the relationship, $\langle S^2\rangle^{1/2} \propto M^{\nu}$.

Figure 9 shows double logarithmic plots of η_R^0 *vs.* C/C^* for P2VP solutions. C^* and $[\eta]$ values for P2VP in a good solvent (pyridine)[1-3] are listed in Table I. The data for PS in αCN and toluene (good solvents) in dilute and semidilute regions[9] are also shown by broken and solid lines, respectively. The features of this figure are the same as those of PS in good solvents. Three low concentration

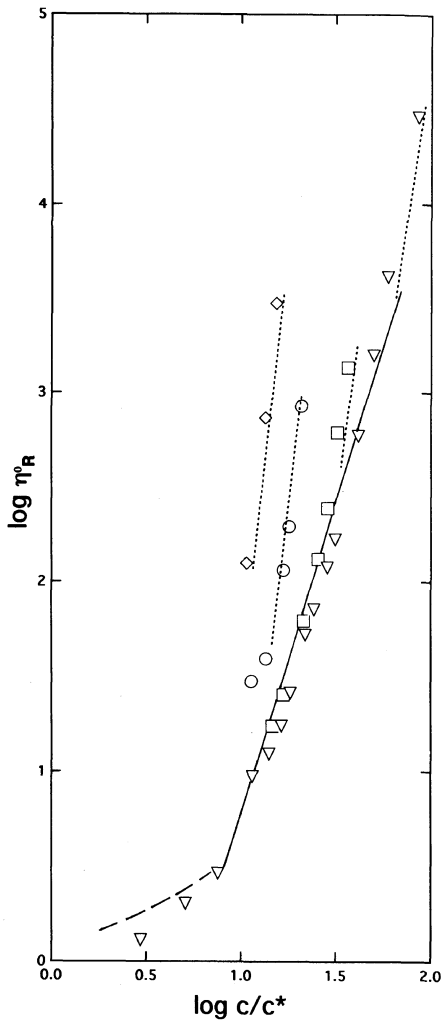

Figure 9. Double logarithmic plots of η_R^0 against C/C^* for P2VP in αCN at 30°C. Symbols are the same as those in Figure 6. Dotted lines denote the data in concentrated region. Broken and solid lines denote the data for PS in good solvents in dilute and semidilute regions, respectively. The slope of solid line is equal to the value calculated from eq 3a with $\nu = 0.59_5$.

data of VPK3 (triangles) are close to broken line. Other data of VPK3 and data of VPL5 (squares) at the concentrations lower than 20 kg dm^{-3} compose a single straight line, while all the data at $C > 20$ kg dm^{-3} cannot be expressed by a universal function of C/C^*, but are represented by different dotted lines with the same concentration dependence. Therefore, the viscosity behavior of P2VP in αCN can be also classified into dilute, semidilute and concentrated regions. The crossover from dilute to semidilute regions occurs at around $C/C^* = 8$ and that from semidilute to concentrated regions occurs at around 20 kg dm^{-3}, which are the same as those for PS in good solvents (toluene and αCN). Both absolute values and C/C^* dependence of η_R^0 in dilute and semidilute regions are almost the same as those of PS in good solvents.[9] Thus, the concentration dependence of viscosity in semidilute region can be well expressed by eq 3 and 3′ (Figures 9 and 6, respectively) with $\nu = 0.59_5$ which is the value used for PS in good solvents.[9] Moreover, the concentration dependence of η_{sp}^0 in the concentrated region shown in Figure 6 is also almost the same as that for PS solutions in αCN.[9] Therefore, it is concluded that both P2VP and PS in αCN exhibit quite

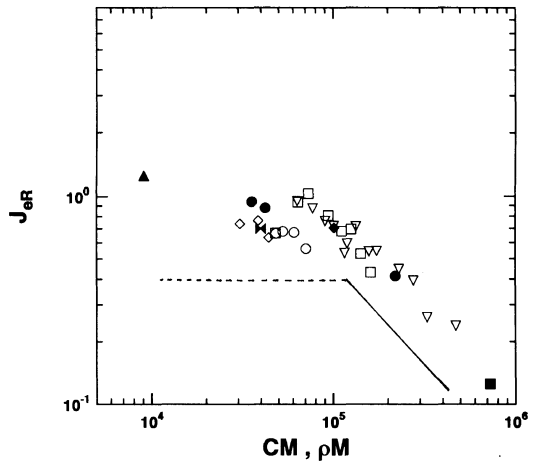

Figure 10. Double logarithmic plots of J_{eR} against CM (or ρM) for P2VP in αCN at 30°C. Filled circles with pips up and right denote the values for VPK21 and VPK22 in bulk, respectively. Other symbols are the same as those in Figures 1 and 6. Filled symbols denote the data in bulk. Dotted and solid lines denote the data for PS in the non-entangled and entangled regions, respectively. The slope of solid line is -1.

similar viscosity behavior. This result also imply that αCN is a common good solvent for both polymers.

Finally, we discuss steady state compliance in solution in terms of reduced steady state compliance J_{eR}, defined by[11,12]

$$J_{eR}=(J_eCRT/M)[\eta^0/(\eta^0-\eta_s)]^2 \quad (4)$$

Figure 10 shows double logarithmic plots of J_{eR} against CM for P2VP solutions at 30°C. The data in bulk is converted to this temperature and also plotted in this figure. The data for PS in non-entangled and entangled regions are denoted by dotted and solid lines, respectively, for comparison. P2VP data are somewhat scattered, but the scattering range is almost the same as that for PS data. In the non-entangled region, J_{eR} is almost constant, while it is inversely proportional to CM in the entangled region. The critical value of CM for entanglement is about 1×10^5, which is equal to the value (M_c') in bulk, and it is slightly lower than that of PS in bulk and solution.[9-12] The absolute values of J_{eR} are slightly higher than those of PS in the whole experimental region.

In summary, we conclude that among various polymers so far studied, poly(2-vinylpyridine) and polystyrene exhibit very similar viscoelastic properties in both bulk and a common good solvent.

REFERENCES

1. Y. Matsushita, K. Shimizu, Y. Nakao, H. Chosi, I. Noda, and M. Nagasawa, *Polym. J. (Tokyo)*, **18**, 361 (1986).
2. Y. Matsushita, Y. Nakao, R. Saguchi, H. Chosi, and M. Nagasawa, *Polym. J. (Tokyo)*, **18**, 493 (1986).
3. Y. Matsushita, Y. Nakao, K. Shimizu, I. Noda, and M. Nagasawa, *Macromolecules*, **21**, 2790 (1988).
4. Y. Matsushita, K. Shimizu, I. Noda, T. Chang, and C. C. Han, *Polymer*, **33**, 2412 (1992).
5. R. G. Larson, *Rheol. Acta*, **31**, 497 (1992).
6. M. Yamaguchi, N. Maeda, Y. Takahashi, Y. Matsushita, and I. Noda, *Polym. J. (Tokyo)*, **23**, 227 (1991).
7. P. G. de Gennes, "Scaling Concepts in Polymer Physics," Cornell University Press, Ithaca, New York, 1979.
8. Y. Takahashi, Y. Isono, I. Noda, and M. Nagasawa, *Macromolecules*, **18**, 1002 (1985).
9. Y. Takahashi, I. Noda, and M. Nagasawa, *Macromolecules*, **18**, 2220 (1985).
10. S. Onogi, T. Masuda, and K. Kitagawa, *Macromolecules*, **3**, 109 (1970).
11. J. D. Ferry, "Viscoelastic Properties of Polymers," 3rd ed, Wiley, New York, N.Y., 1980.
12. W. W. Graessley, *Adv. Polym. Sci.*, **16**, 1 (1974).
13. K. Mori, Master Thesis, Nagoya University, 1988.
14. Y. Isono, T. Fujimoto, T. Takeno, and M. Nagasawa, *Macromolecules*, **11**, 888 (1978).